Aviation Gasoline Quality Detection Using RAP Feature Selection and IMPA-XGBoost Optimization

Yong Zhang[1*], Yadi Peng[2], Guoteng Hui[1]
[1]School of Computer Science, Civil Aviation Flight University of China, Guanghan 618300, China
[2]Aviation Fuel Management Office, Civil Aviation Flight University of China, Guanghan 618300, China
E-mail: gnoygnahz11@163.com, nancyyadias@163.com, huiguoteng@126.com
*Corresponding author

Keywords: XGBoost, IMPA, aviation gasoline, quality detection, RAP

Received: March 29, 2025

Quality detection of aviation gasoline is critical to flight safety. Gasoline is a critical fuel for aircraft engines, and any quality problem may affect the performance of the engine and the safety of the aircraft. Regarding the issue of aviation gasoline detection, a RAP method combining Pearson correlation coefficient method and Relief-F algorithm is studied for gasoline mass spectrometry feature selection. Improved marine predator algorithm (MPA) introduces Logistic chaotic mapping and adaptive t-distribution operator. It is used to optimize the XGBoost model to construct an aviation gasoline quality detection model for gasoline quality detection and model classification. Among them, the RAP method is chosen because it effectively removes redundant features from mass spectrometry data while preserving the correlation between features. The use of IMPA to optimize XGBoost is because the traditional MPA is easy to fall into local optimum. Whereas the improved IMPA can find the optimal hyperparameter combination of XGBoost more effectively by enhancing the population diversity and optimizing the search strategy, thus improving the model detection performance. The results showed that the area under the receiver operating characteristic curve (AUC) of the proposed model was 0.8892, which was significantly higher than the AUC values of the particle swarm optimization-XGBoost (PSO-XGBoost) model (0.8384) and the sparrow search algorithm-XGBoost (SSA-XGBoost) model (0.8497). In the classification of gasoline models, only 4 samples were misclassified, while 122 samples were classified correctly, with an accuracy rate of 96.83%. This was a significant improvement compared to the 92.06% of the SSA XGBoost model and the 88.10% of the PSO XGBoost model. The improved marine predator and extreme gradient boosting model has shown excellent performance in gasoline quality detection. Compared to traditional chemical detection methods, such as plasma emission spectroscopy and gas chromatography with an oxygen-selective detector, the AI-based detection system proposed in this study has significant advantages in terms of detection accuracy and efficiency, and does not require expensive and complex detection equipment. This provides a strong support for AI automated system in quality detection of aviation gasoline.

Povzetek: Študija predstavlja RAP (Relief-F + Pearson) za izbor masnospektrometričnih značilk ter IMPA-optimiziran XGBoost za zaznavanje kakovosti letalskega bencina.

1 Introduction

The importance of airplane flight safety has increased with the aviation industry's explosive growth. The quality detection of aviation gasoline plays a crucial role in flight safety. Therefore, it is necessary to adopt effective quality detection methods to ensure that the quality of aviation gasoline meets the specifications [1]. Traditional gasoline detection methods include plasma emission spectrometry, gas chromatography oxygen selective detector (GC-OD) method and other chemical experimental methods [2]. In aviation gasoline, silicon is the residue left behind after combustion. This residue accelerates the wear and tear of pumps, valves, etc. For this reason, scholars have used plasma emission spectrometry to measure silicon content in gasoline in an attempt to determine its quality and type. Alcohols and other oxygenates can be added to gasoline. However, adding too many oxygenates affects the performance and efficiency of gasoline engines and causes environmental pollution. For this reason, GC-OD is used to determine the content of C7 ether and other ether compounds in gasoline, and then to realize the detection and model classification of gasoline quality. However, this type of chemical detection method requires high cost of detection equipment, difficult operation, and limited detection range [3-4]. As a result, numerous researchers have begun to seek more efficient and automated detection solutions. Advances in artificial intelligence and automated systems in recent years have provided new ideas for detecting the quality of aerogasoline. Especially in the field of machine learning (ML), the eXtreme gradient boosting (XGBoost) model has been widely used in various data analysis tasks due to its efficient performance [5-6].

XGBoost is widely used in detection and prediction in various fields. For chiller unit defect diagnosis and detection, Zhang et al. integrated a parameter-optimized XGBoost model with a mean-drift clustering technique, resulting in a multi-region XGBoost model. The findings showed that the model outperformed the support vector machine model and the XGBoost model without clustering in terms of defect diagnosis rate. It was able to detect 97.26% of faulty samples and was able to detect 99.10% of fault-free samples [7]. Chen et al. proposed XGBoost model for the study of self-recognition technical debt classification in software development. The method employed a trained XGBoost classifier to classify each comment into the corresponding class. The outcomes demonstrated that the average accuracy of the proposed method under study was 56.66%, the average recall was 59.07% and the average F1 value was 55.77%. Its improvement was 4.98%, 5.32% and 3.17% compared to natural language processing-based methods [8]. Qiu et al. proposed an optimized XGBoost model with whale optimization algorithm to optimize its hyperparameters in order to detect the ground vibration caused by blasting. The results demonstrated that the XGBoost model based on the whale optimization algorithm had the lowest error value compared with the rest of the artificial intelligence algorithms. The root mean square error was only 3.0538 and the mean absolute error was only 2.5032 [9]. Asselman et al. proposed a performance factor analysis method based on the XGBoost model in order to enhance the prediction performance of student performance. The outcomes showed that the performance of scalable XGBoost proposed by the study had superior predictive performance compared to traditional performance factor analysis algorithms [10].

In recent years, the traditional marine predator algorithm (MPA) algorithm has been improved in various fields to enhance the application. Ramezani et al. found that the traditional MPA could not produce diverse initial populations with high productivity and optimized it using a dyadic-based learning approach with chaotic mapping method. The results indicated that the improved MPA proposed by the study provided better performance compared to particle swarm optimization algorithm, whale optimization algorithm, etc. In the real-world optimization problem for DC motors [11]. An enhanced MPA based on the sine-cosine algorithm was proposed by Abd Elaziz et al. for the feature selection problem for high dimensional data. To maximize the search capacity, the method used the sine-cosine algorithm as a local search of the original MPA. According to the findings, the enhanced MPA performed noticeably better in terms of categorization metrics [12]. To address the issue of resource waste brought on by an uneven node distribution in distributed network systems, He et al. suggested an enhanced MPA method. According to the findings, the enhanced MPA had a higher coverage rate than other meta-heuristic algorithms when resolving the issue of distributed network system coverage optimization [13]. For interdisciplinary data analysis, Jia et al. proposed an MPA based on co-evolutionary cultural mechanisms. The algorithm could realize the sharing of knowledge and experience in different spaces. The results indicated that the MPA based on the co-evolutionary cultural mechanism outperformed the remaining advanced data analysis methods in several evaluation metrics [14].

The study compared the performance of the proposed method with that of existing advanced methods, including global context-outlier detection (GC-OD), principal component analysis+extreme gradient boosting (PCA+XGBoost), and whale optimization algorithm+extreme gradient boosting (WOA-XGBoost). The comparison results are shown in Table 1. Although GC-OD has high feature selection robustness, it has a long running time and is not suitable for large-scale datasets. Although PCA+XGBoost offers dimensionality reduction and powerful classification capabilities, its feature selection is not precise enough, which can easily result in the loss of important information. Although WOA-XGBoost has strong optimization capabilities, it is prone to getting stuck in local optima and has a slow convergence speed. In contrast, the proposed IMPA-XGBoost method outperforms existing methods in key indicators such as the area under the curve (AUC), F1 value, and recall rate. It also demonstrates excellent robustness and runtime in feature selection.

Table 1: Performance comparison between existing advanced methods and the proposed method

Method	AUC	F1	Recall	Sample size	Feature selection robustness	Run time
GC-OD	0.82	88.5%	85.0%	500	Tall	Slow
PCA+XGBoost	0.85	90.0%	87.0%	300	Centre	Medium
WOA-XGBoost	0.84	89.5%	86.0%	200	Centre	Medium
The proposed method (IMPA-XGBoost)	0.8892	96.83%	94.86%	420	Tall	Fast

In summary, researchers at home and abroad have carried out numerous studies on the improvement and application of XGBoost model and MPA in various fields. However, few studies have applied the combination of the two to the detection of aviation gasoline. For this reason, the study innovatively applies the two together in the quality detection and classification of aviation gasoline, using XGBoost classification algorithm for gasoline quality detection. Meanwhile, the improved marine predator algorithm (IMPA) is proposed on this basis, and

a gasoline quality detection model based on IMPA-XGBoost is developed in order to guarantee aviation safety. By proposing this model, the research aims to address three key issues. First, it is necessary to clarify whether the RAP method can effectively reduce the feature dimensions of aviation gasoline mass spectrometry data without sacrificing accuracy. Second, it is important to determine if the IMPA is more effective than optimization algorithms, such as PSO and SSA, at finding the optimal hyperparameter combination for XGBoost. Finally, verify whether the IMPA-XGBoost-based model can detect aviation gasoline quality and classify models more accurately and efficiently. Model performance is evaluated based on success criteria such as detection accuracy, AUC value, and running time. If the model outperforms existing methods in these indicators, it is considered that the research has achieved the expected goals. The innovation of the study is to optimize the improved IMPA to address the problem of low detection rate of XGBoost in gasoline quality detection. The optimized method can find the best parameter combination in a shorter time and can reduce the consumption of computational resources, making the detection process more efficient and reliable.

2 Methods and materials

In quality detection of aviation gasoline, the study begins with gasoline mass spectrometry using seven standard gasoline samples, followed by feature selection of the mass spectrometry data using the Relief-F algorithm-Pearson correlation coefficient (RAP). Subsequently, the XGBoost algorithm is introduced and the combination of hyperparameters for this algorithm is determined using the IMPA. Among them, for the optimization of the MPA, logistic chaos mapping with adaptive t-distribution operator is introduced. Finally, the gasoline quality detection model based on IMPA-XGBoost is constructed.

2.1 RAP-based feature selection for gasoline mass spectrometry

To achieve quality detection of aviation gasoline, seven standard gasoline samples are selected for mass spectrometry analysis for subsequent quality detection and model identification. These include 89.0#, 90.4#, 91.0#, 92.4#, 93.9#, 95.2#, and 99.4#. The mass spectrometry method used is paper spray ionization, which mainly analyzes mass spectrometry data in the positive ion mode. Each gasoline model contains 60 mass spectrometry data with a total of 420 data. The model's ability to identify chemical characteristic variations is fully verified by the significant differences in octane number, oxygen-containing compounds, and impurity content among different grades of gasoline. Due to the involvement of industry standards in aviation fuel data, it is currently not possible to fully disclose it. However, the samples used in the experiment are purchased from Standard Products, which is certified by the China Aviation Fuel Testing Center. The testing process strictly followed GB/T 35394-2017, "General Specifications for Spectral Testing of Aviation Fuel," to ensure data traceability and standardization. The study takes the 89.0# gasoline model as an example, and lists two sets of these mass spectrometry data, as shown in Table 2. Mass denotes the mass to charge ratio (MCR) of the ion. Relative intensity denotes the relative intensity, i.e., the MCR of the ion in the sample. The sample numbers "-6" and "-7" represent the 6th and 7th independent mass spectrometry samples collected from 89.0 # gasoline.

Table 2: Two sets of mass spectrometry data for 89.0 # gasoline.

89.0#-6		**89.0#-7**	
Mass	Relative Intensity	Mass	Relative Intensity
50.559415	4.286951	50.642162	23.36641
51.268943	487.6285	51.296954	645.3361
52.269449	109.3655	52.169842	150.3496
53.385469	9822.364	53.354994	11392.63
54.359625	729.6651	54.167274	622.3644
...	...	...	...

In Table 2, the raw mass spectrometry data has high relative intensity values. If left unprocessed, the features with lower intensities would be ignored. For this reason, the study used the maximum-minimum normalization method to normalize the raw data so that the range of relative intensity values is controlled between [0, 1]. The normalization processing formula is shown in Equation (1).

$$q_{new} = \frac{q - q_{\min}}{q_{\max} - q_{\min}} \tag{1}$$

In Equation (1), q denotes the original relative intensity value. $q_{\max}$ denotes the original relative intensity maximum value. $q_{\min}$ denotes the original relative intensity minimum value. q_{new} denotes the normalized relative intensity value. To make subsequent processing more convenient, the normalized data is enlarged tenfold to control the relative intensity range between 0 and 100. This retains relative differences in features while avoiding neglecting small value features. The schematic mass spectral images of 89.0 #6 gasoline before and after normalization are shown in Fig. 1.

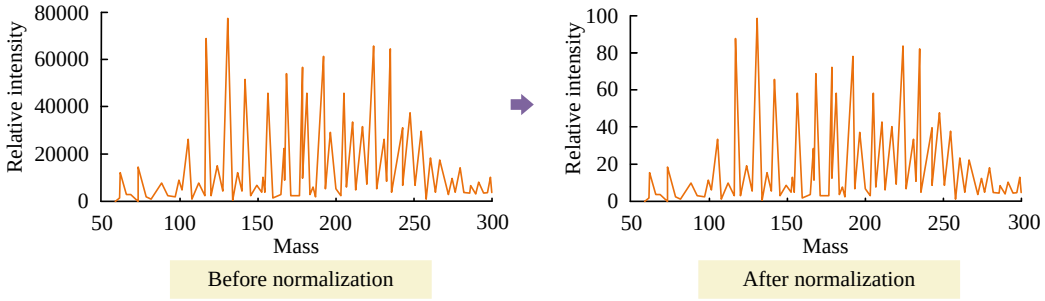

Figure 1: Schematic diagram of mass spectrometry images before and after normalization of 89.0 # 6 gasoline.

The MCR of gasoline mass spectrometry data ranges from 50-500 and contains 450 features. If all the features are directly used for model training, there will be problems such as long running time and low detection accuracy. To extract useful characteristics from the data and eliminate superfluous features, the study presents the Relief-F algorithm. In this case, the main basis for the assignment of weights is the contribution of the sample. After assigning values to the weights, they need to be ranked. The top ranked features are of greater importance and have the priority of selection [15-16]. In Relief algorithm, it is assumed that a sample is randomly selected and the near neighbor samples of this sample can be classified as similar samples and dissimilar samples. The weights of Relief algorithm are calculated as shown in Equation (2).

$$W[B] = \sum_{p} -diff(B, R_o, H_p) + diff(B, R_o, M_p) \quad (2)$$

In Equation (2), B represents a randomly selected sample. R_o represents the nearest neighbor sample belonging to the same class as sample B. H_p and M_p represents the p-th sample belonging to the same class as sample B, and the sample belonging to a different class from sample B. $diff(\cdot)$ represents the diversity of the sample. All samples in the equation are n-dimensional vectors, where n is the total number of features. Since the traditional Relief algorithm can only solve the binary classification problem, the study further employs the improved Relief-F algorithm. This algorithm needs to find a number of similar and dissimilar near-neighbor samples when weighting a certain sample, which is suitable for multiclassification problems. In addition, although the Relief-F algorithm has high computational efficiency when performing feature screening, it ignores the correlation between features and features, which is not conducive to feature classification. Meanwhile, there may be many repeated information in the screened features. If they are not eliminated, the training accuracy of the subsequent quality detection model will be affected [17]. For this reason, the study further adopts RAP and proposes a RAP-based feature selection algorithm for gasoline mass spectrometry. Among them, the Pearson correlation coefficient (PCC) method has important applications in feature selection and data preprocessing. Especially when dealing with high-dimensional datasets, it can effectively remove redundant features and reduce the multicollinearity problem. The computational expression of PCC method is shown in Equation (3).

$$r_{BB'} = \frac{\sum_{a=1}^{A}(B_a - \bar{B})(B'_a - \bar{B}')}{\sqrt{\sum_{a=1}^{A}(B_a - \bar{B})^2}\sqrt{\sum_{a=1}^{A}(B'_a - \bar{B}')^2}} \quad (3)$$

In Equation (3), C denotes the total samples. B_c and B'_c denote the two samples with serial numbers. $\bar{B}$ and $\bar{B}'$ denote the sample mean. The flowchart of the RAP-based feature selection algorithm for gasoline mass spectra is shown in Fig. 2. The Relief-F algorithm is first used to calculate the MCR weights and determine the relative importance of each feature. Then the PCC method is used to further calculate the relative coefficients of the features in the subset. For several features with higher relative coefficients, one feature with higher weight is retained. For the features with lower relative coefficients, they are all retained in the final feature set.

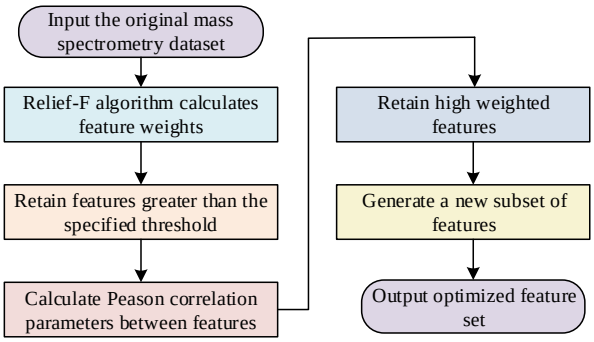

Figure 2: Flowchart of RAP based gasoline mass spectrometry feature selection algorithm.

2.2 Gasoline model recognition model based on XGBoost

After normalization of gasolinemass spectrometry data as well as feature selection, the study further constructs gasoline quality detection model, from which the XGBoost classification algorithm is introduced. The algorithm is a ML algorithm based on the gradient boosting framework, and the base model of the XGBoost classification algorithm is assumed to be a CART regression tree. Its expression is shown in Equation (4) [18].

$$\hat{y}_a = \sum_{l=1}^{L} f_l(x_a) \quad (4)$$

In Equation (4), $f_l(x_a)$ represents the weight value of the a th sample of the l th tree. l represents the index of the l -th tree. a represents the index of sample a. Each tree can output predicted values for all samples, and then accumulate them to obtain the ensemble prediction result of the samples. $\hat{y}_a$ represents the prediction result of the base model for the a th sample. L denotes the number of CART trees. The resulting expression for the objective function is shown in Equation (5).

$$Obj(\theta) = \sum_{a=1}^{A} loss(\hat{y}_a, y_a) + \sum \Omega(f_l) \quad (5)$$

In Equation (5), y_a represents the true value of the a th sample. $loss(\hat{y}_a, y_a)$ represents the loss error and $\Omega(f_l)$ represents the regularity term. The expression of $\Omega(f_l)$ is shown in Equation (6).

$$\Omega(f) = \gamma T + \frac{1}{2}\lambda w^2 \quad (6)$$

In Equation (6), γ and λ denote the penalty coefficients. T is the number of nodes. w denotes the corresponding weight value. The resulting objective function is shown in Equation (7).

$$Obj(\theta) = \sum_{a=1}^{A} loss\left(y_a, \hat{y}_a^{(t-1)} + f_t(x_a)\right) + \Omega(f_t) + Const \quad (7)$$

In Equation (7), *Const* denotes the constant term. $\hat{y}_a^{(t-1)}$ represents the predicted value of the base model for the $t-1$-th sample during the $t-1$-th iteration. After the second order Taylor expansion, the computational equation is obtained as shown in Equation (8).

$$Obj(\theta) = \sum_{t=1}^{T}[G_t w + \frac{1}{2}\lambda w_t^2] + \gamma T \quad (8)$$

In Equation (8), G_t is calculated as shown in Equation (9).

$$G_t = \sum \partial \hat{y}^{(t-1)} loss(y_a, \hat{y}_a^{(t-1)}) \quad (9)$$

$\hat{y}_a^{(t-1)}$ is mainly derived from the initial value setting and the accumulation of historical information during the iteration process. The calculation after derivation of w_t is shown in Equation (10).

$$w_t = -\frac{G_t}{\lambda} \quad (10)$$

Substituting w_t into Equation (10) leads to Equation (11).

$$Obj(\theta) = -\frac{1}{2}\sum_{t=1}^{T}\frac{G_t^2}{\lambda} + \lambda T \quad (11)$$

Equation (11) is the final XGBoost algorithm objective function. In the XGBoost algorithm, the selection of hyperparameters is crucial. The traditional grid search method suffers from time-consuming and ineffective problems in performing parameter selection [19]. For this reason, the study introduces the MPA for hyperparameter combination determination to improve the recognition accuracy of gasoline quality detection model. The MPA simulated the food relationship of different marine organisms as a way to solve the optimization problem. However, the algorithm is more sensitive to the initial value of the problem and is easy to fall into the local optimal solution, so it often cannot solve the optimization problem alone. In the performance optimization process of the population intelligence algorithm, the diversity of the population has an important impact on the quality of the final results. If the individual positions of the initial population are too concentrated, it will cause the algorithm to fall into a local optimum and cannot fully explore the whole search space [20]. To enhance the diversity of the population and to improve the global optimization ability of the algorithm, the study introduces Logistic chaotic mapping. It is a kind of quadratic polynomial mapping, shooting with high randomness and low computational cost, which is easy to implement. The approach in population optimization can cover the search space more thoroughly and prevent an undue concentration of population members in the search space [21]. Because of this, the study initializes the MPA's population using logistic chaotic mapping. Equation (12) displays its expression.

$$X_{k+1} = \mu x_k (1 - x_k) \quad (12)$$

In Equation (12), the value range of x is (0, 1]. k denotes the current iteration number. μ denotes the control parameter. When μ is in the range of (3.5699,4.0), the sequence enters a chaotic state. When $\mu = 4$, the population becomes more random, which allows it to cover the search space more comprehensively, avoid getting stuck in local optima, and distribute itself more uniformly at the beginning. Therefore, the study set $\mu = 4$. In the traditional MPA, the relationship between predator and prey simulates the predatory behavior in nature. The predator represents the solution or individual in the algorithm, while the prey is the goal or individual in the environment that needs to be optimized. The predator searches by following the position of the prey, thus gradually approaching the optimal solution. Predator positions must be modified in accordance with changes in prey positions. To update the solution after the prey's position changes, the study introduces an adaptive t-distribution operator. This operator generates high-quality potential positions in the solution space with a high probability through its specific probability density function. Equation (13) displays the representation of the mathematical model.

$$X_i^{'} = X_i + X_i \bullet t(Iter) \quad (13)$$

In Equation (13), $t(Iter)$ is the t-distribution. X_i represents the original prey position. $X_i^{'}$ represents the updated prey position. In this study, the degree of freedom of the adaptive t-distribution operator is set to 3. This value is determined through preliminary experiments within the range of [1, 10] with a step size of 1. Then, 10-fold cross-validation is used to evaluate the performance of the IMPA-XGBoost-based gasoline quality detection model under different degrees of freedom. The steps of the improved IMPA are shown in Fig. 3.

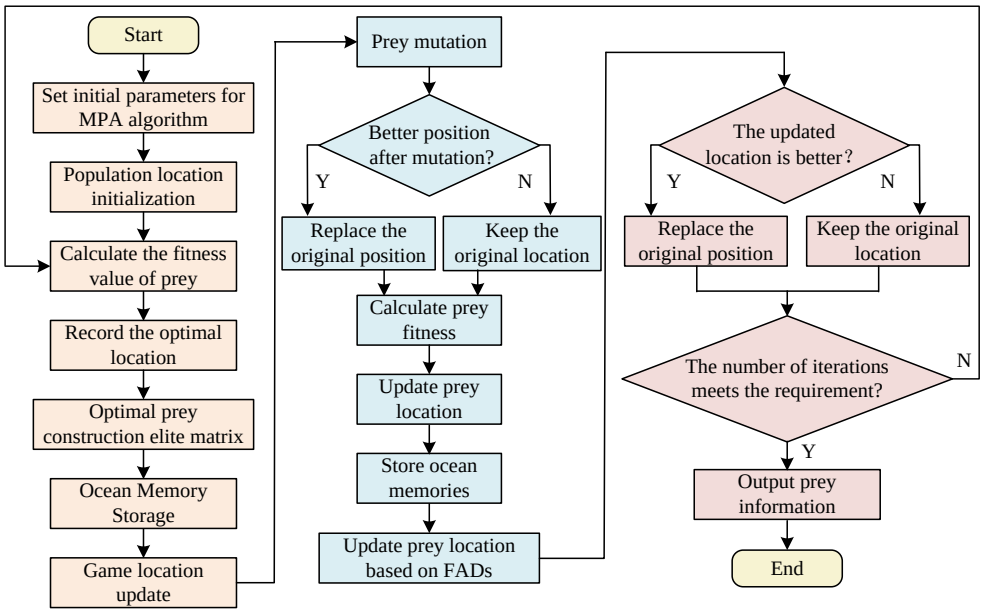

Figure 3: Complete iterative flowchart of IMPA based on chaotic mapping and adaptive strategy.

The basic XGBoost algorithm has many hyperparameters, once a parameter is set incorrectly, it will affect the detection accuracy of the whole model, so the hyperparameters of this algorithm need to be adjusted. The parameters used in the study include eta, max_depth, n_estimators, and gamma. Among them, eta denotes the learning rate and is used to control the learning rate. max_depth denotes the maximum depth of the tree. Its value should not be too large. Otherwise, it will lead to overfitting. The n_estimators denotes the trees, and gamma is mainly responsible for controlling the minimum loss reduction of the leaf nodes of the decision tree. In addition, the fitness function of gasoline quality detection model is calculated as shown in Equation (14).

$$fitness = \frac{1}{10}\sum_{e=1}^{10} accuracy_e \tag{14}$$

In Equation (14), *accuracy* denotes the average of the accuracy of the samples in the validation set. 10 denotes that the function is 10-fold cross-validation. After determining the hyperparameters and ranges to be optimized, the gasoline quality detection model based on the IMPA-XGBoost algorithm is then constructed. The flowchart of the model is shown in Fig. 4.

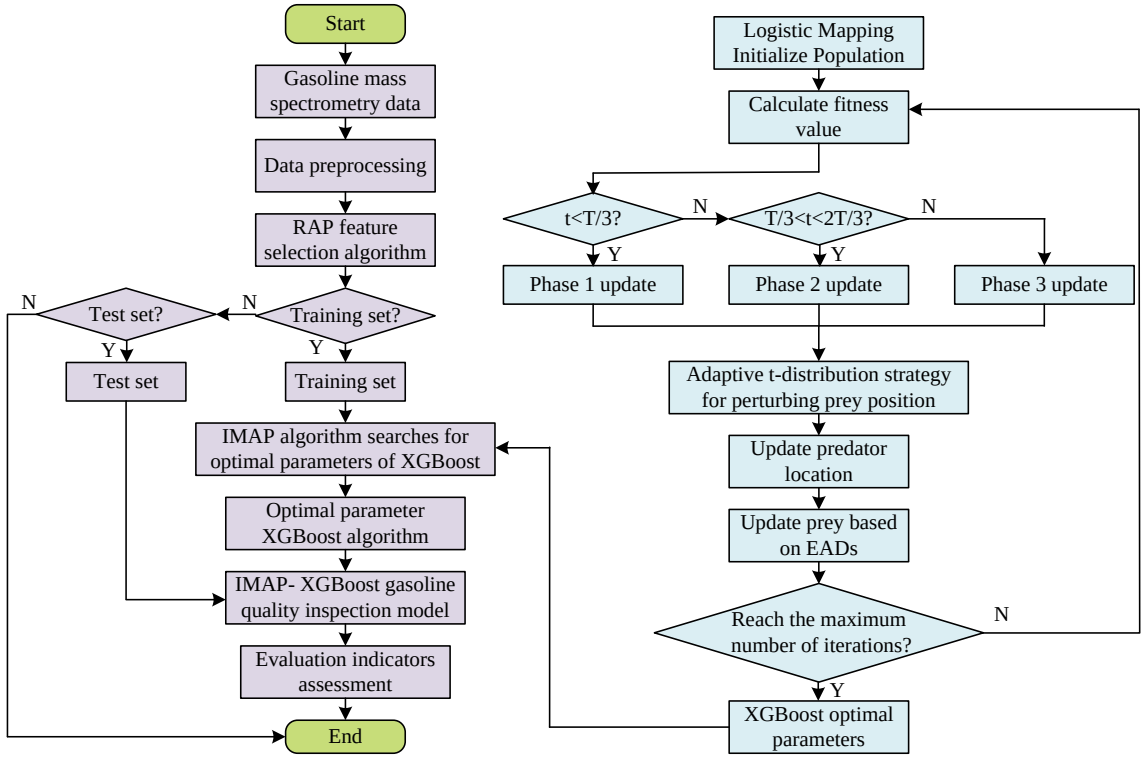

Figure 4: Step by step implementation from mass spectrometry data preprocessing to IMPA-XGBoost model evaluation.

In Fig. 4, the mass spectrometry data of seven standard gasoline samples are first used as the basis, and the data range is unified through preprocessing. Then, the RAP feature selection algorithm is used to streamline features and remove redundancy. Next, according to the dataset type, the IMPA is used to search for the optimal hyperparameters of XGBoost, and an IMAP XGBoost detection model is constructed. Finally, the performance of the model is validated through evaluation indicators.

3 Results

The study firstly verifies the effectiveness of RAP-based feature selection using Relief-F algorithm with blank group to compare with it. Then the effectiveness of gasoline quality detection model based on IMPA-XGBoost algorithm is verified. Its accuracy, loss value in the training phase is analyzed and area under curve (AUC) with gasoline model classification accuracy (CA) during testing is verified.

3.1 Experimental analysis of RAP-based feature selection

The computing environment used in the experiment is Intel Xeon Silver 4310 CPU (32GB memory), Ubuntu 20.04 system, relying on Python 3.9+XGBoost 1.7.6 and other libraries. The environment is encapsulated with Docker images to ensure reproducibility. The study first adopts the Relief-F algorithm to calculate the weights of the preprocessed gasoline mass spectrometry data. The feature subset is selected to be MCR with a weight value greater than 0.14, and a total of 20 MCR features are screened. The selection of threshold 0.14 is mainly determined through the grid search method of the system. Subsequently, PCC method is used to analyze the correlation of the feature subset, and the PCC plot with the final feature subset is shown in Fig. 5. In Fig. 5(a), if the correlation between the horizontal and vertical coordinates of the two features tends to 1, they indicate a strong positive correlation. If the correlation tends to -1, it shows a sharp negative correlation color. Both cases indicate that the two features have a strong correlation relationship and one needs to be eliminated. If the correlation between the two feature color blocks remaining 0, it means that the two do not have correlation, both need to be retained. In Fig. 5(a), every two features with MCR of 177, 191, 202, 216, 230, 231, 232, and 244 are strongly correlated. Finally, 221 is retained, which has the highest weight value. Every two features in the features with MCR of 100, 114, 115, 128, 168 are strongly correlated. The feature with MCR of 114 is finally retained. Every two features in the features with MCR of 142, 154, 156 are strongly correlated and finally the feature with MCR of 154 is retained. The correlation coefficient between features with MCR of 69 and 83 is greater than 0.9, and 69 is finally retained. In addition, features with low correlation are retained, resulting in the final subset of features, as shown in Fig. 5(b).

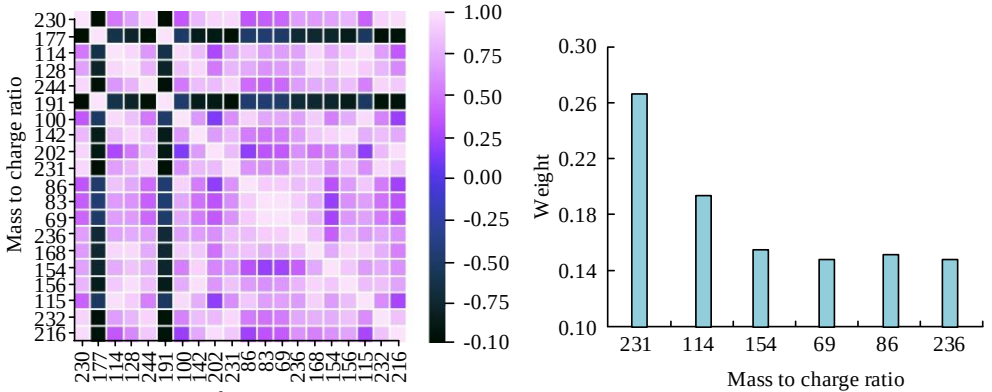

(a) Pearson correlation coefficient chart

(b) Final feature subset of gasoline mass spectrometry data

Figure 5: Pearson correlation coefficient plot and final feature subset.

The study then proceeds to perform quality testing on gasoline mass spectrometry data, using stratified sampling to divide the training set into a 70% training set and a 30% testing set. Samples of the same type of gasoline are dispersed evenly between the training and testing sets rather than being grouped together. Specifically, 60 data points are shuffled for each type of gasoline according to random seeds. The first 42 points are selected as the training set, and the last 18 points are selected as the testing set. This avoids model bias caused by uneven sample allocation. In addition to the 70-30 segmentation, 10-fold stratified cross-validation is introduced during the RAP feature selection and IMPA-XGBoost training stages. The feature set filtered by RAP will be divided into ten subsets by label. The model will then be trained on nine of the subsets and validated on the tenth subset, one at a time. The average of the 10 validation results will be taken to evaluate the stability of the model. To verify the effectiveness of the RAP-based feature selection algorithm, the study adopts Relief-F algorithm to compare with it. Moreover, a blank group without feature algorithm is set up to analyze the accuracy, recall and F1 value of gasoline quality detection under the three schemes. The performance of gasoline quality detection under different feature selection schemes is shown in Fig. 6. In Fig. 6(a), the accuracy of RAP-based feature selection algorithm is 97.26% on average, while the accuracy of Relief-F algorithm is only 85.16%. The accuracy of the blank group without feature selection is only 81.03%. In Fig. 6(b), the average recall of the RAP-based feature selection

algorithm is as high as 94.86%, which is a 10.81% improvement compared to the Relief-F algorithm. In Fig. 6(c), the average F1 value of RAP-based feature selection algorithm is as high as 96.23%, which is improved by 17.63% compared to the blank group. It indicates that the RAP-based feature selection algorithm is beneficial to improve the performance of gasoline quality detection. By optimizing the feature set, it can reduce the effects of redundant information and noise, making the model better able to capture important gasoline quality information throughout the testing phase.

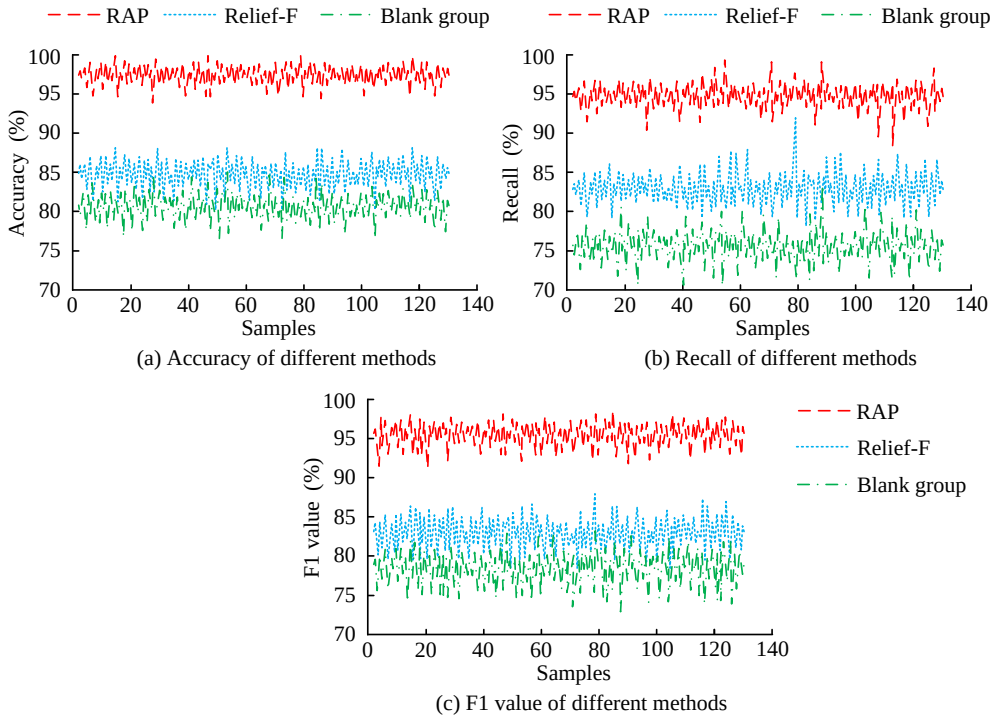

(a) Accuracy of different methods

(b) Recall of different methods

(c) F1 value of different methods

Figure 6: Performance of gasoline quality detection under different feature selection schemes.

To verify the significant advantages of the RAP feature selection algorithm, an independent sample t-test is performed to statistically analyze the detection performance of RAP and Relief-F. The results are shown in Table 3. According to Table 3, the RAP algorithm achieves a significantly higher accuracy index (97.26%±1.35%) than Relief-F (85.16%±2.47%, p<0.001). In terms of F1 score, RAP is as high as 96.23%±1.12%, while Relief-F is only 87.34%±1.89%, with a significant statistical difference between the two (p<0.001). On the Matthews correlation coefficient (MCC) metric, the RAP algorithm achieves 93.57%±1.28%, significantly higher than Relief F's 78.62%±2.35% (t=6.12, p<0.001). This indicates that the RAP algorithm has a statistically significant advantage in feature selection performance. Combining it with the PCC method effectively improves model performance by removing redundant features.

Table 3: The t-test results of RAP and Relief-F feature selection methods.

Index	RAP	Relief-F	*t*	*p*
Accuracy	97.26%±1.35%	85.16%±2.47%	5.72	<0.001
Recall	94.86%±1.52%	84.05%±2.11%	5.36	<0.001
F1 value	96.23%±1.12%	87.34%±1.89%	4.91	<0.001
MCC	93.57%±1.28%	78.62%±2.35%	6.12	<0.001

The study proceeds to validate the gasoline quality detection runtime of each method and the runtime of each algorithm is shown in Fig. 7. The average running time of the gasoline detection model is only 386.69ms after feature selection using the RAP algorithm, which is 362.81ms shorter than that of the Relief-F algorithm. In the blank group without feature selection, the average running time of the gasoline detection model is as high as 160.38ms. It indicates that the feature selection algorithm based on the RAP algorithm not only improves the detection accuracy of the gasoline detection model, but also reduces the detection time of the model. The reason is that the RAP algorithm effectively filters out the most discriminative features. This reduces the amount of data the model must process, thereby reducing the computational burden and running time. In addition, the RAP algorithm avoids the interference of redundant and irrelevant features by optimizing the feature selection process, which enables the model to make decisions more quickly at runtime.

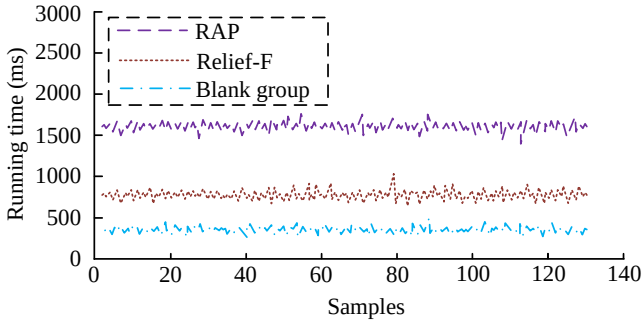

Figure 7: The running time of gasoline quality testing for various methods.

3.2 Experimental analysis of gasoline quality detection based on IMPA-XGBoost algorithm

To verify the effectiveness of the proposed gasoline quality detection model based on IMPA-XGBoost algorithm, the study uses particle swarm optimization-XGBoost algorithm (PSO-XGBoost) and sparrow search algorithm-XGBoost algorithm (SSA-XGBoost) are used for performance comparison. Among them, the population size of the IMPA is 50, the maximum number of iterations is 100, the value of μ in the Logistic chaotic map is 4, and the degree of freedom of the adaptive t-distribution is 3. Based on the outcomes of various algorithms' quality detection tests, the gasoline models are grouped. Table 4 displays the hyperparameter optimization outcomes for each algorithm in comparison to the XGBoost algorithm.

Table 4: The hyperparameter optimization results of various algorithms for XGBoost algorithm.

Hyperparameters	Search scope	PSO-XGBoost	SSA-XGBoost	IMPA-XGBoost
eta	[0.01, 1.0]	0.825	0.751	0.782
max_depth	[3, 15]	9	6	5
n_estimators	[10, 100]	38	27	20
gamma	[0, 1]	0.2	0.1	0

The study substitutes the obtained algorithmic hyperparameters into each algorithm and verifies the training accuracy and loss rate of each model in the gasoline mass spectrometry data training set for analysis. The outcomes are shown in Fig. 8. In Fig. 8(a), the gasoline quality detection model based on IMPA-XGBoost algorithm tends to have an accuracy of 99% at 18 times of training. Although the SSA-XGBoost model fluctuates significantly during the pre-training period, it stabilizes after 50 iterations. Its accuracy then stabilizes at 92.56%. When the PSO-XGBoost model is iterated about 65 times, its accuracy tends to be 90.21%. In Fig. 8(b), the loss rate of the IMPA-XGBoost model tends to be 3.41% when it is iterated up to about 8 times, whereas the SSA-XGBoost model tends to be stabilized only when it is iterated up to about 40 times, and its minimum loss rate is 9.68%. The PSO-XGBoost model converged to 5.18% at 36 iterations. The proposed IMPA-XGBoost model of the study shows higher CA and lower loss rate in the training set with high stability and convergence efficiency.

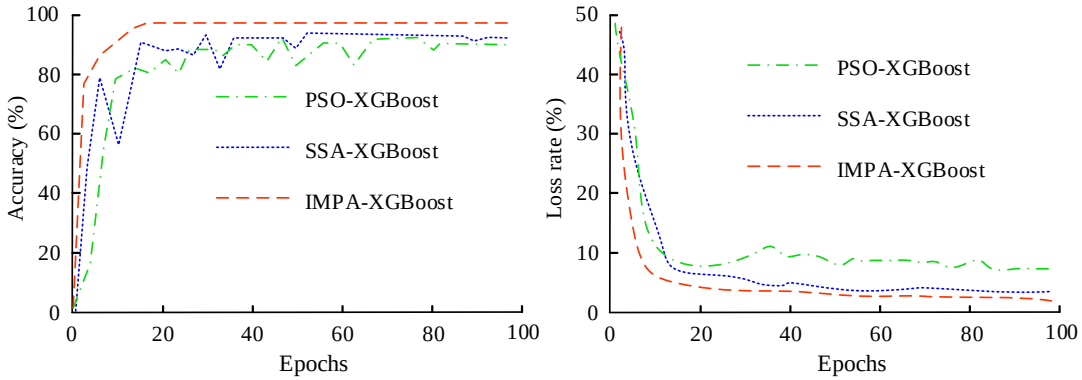

(a) Accuracy of different algorithms (b) Loss rate of different algorithms

Figure 8: Training accuracy and loss rate of each model.

The study continues to measure the quality detection performance of the IMPA-XGBoost models using AUC values. The AUC value reflects the model's ability to distinguish between different quality categories of

gasoline. The closer the value is to 1, the greater the model's sensitivity and specificity in identifying positive and negative samples under various classification thresholds. This indicator is highly consistent with the aviation gasoline quality testing target and is key to measuring the proposed model's performance. The receiver operating characteristic curve (ROC) curves for each model are shown in Fig. 9. Among them, the y-axis represents the true positive rate, which is the proportion of correctly identified positive classes. The x-axis represents the false positive rate, which is the proportion of incorrectly identified negative classes. The closer the AUC is to 1, the better the classification performance. The IMPA-XGBoost model has the highest AUC value of all of the detection findings, at 0.8892 (95% CI: 0.8721-0.9035). In contrast, the AUC values of the SSA-XGBoost and PSO-XGBoost models are lower, at 0.8497 (95% CI: 0.8312-0.8659) and 0.8384 (95% CI: 0.8197-0.8543), respectively, than the IMPA-XGBoost model. It shows that the IMPA-XGBoost model can better distinguish different gasoline quality categories in the classification task. The high AUC values reflect that the model maintains high sensitivity and specificity under various classification thresholds, which proves its reliability and effectiveness in practical applications. It shows that the proposed IMPA-XGBoost model of the study has significant performance advantages in gasoline quality detection.

The study further classifies the models based on the gasoline quality detection results of the models and explores the CA of each model.

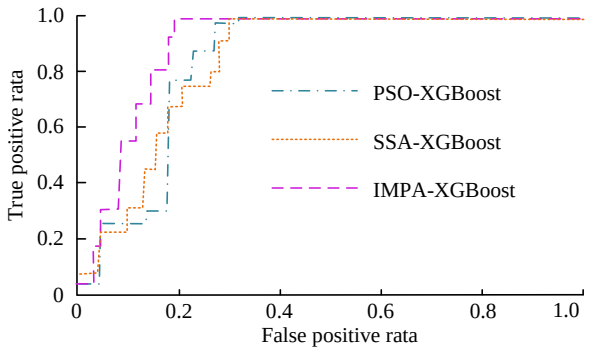

Figure 9: ROC curves of various models.

The CA can intuitively reflect the correctness of the model's gasoline quality inspection results. The model's high accuracy means it can more reliably identify the type and quality of gasoline, helping to reduce flight safety hazards caused by misjudgments. The CA of each model for gasoline models is shown in Fig. 10. In Fig. 10(a), only 4 samples are misclassified in the IMPA-XGBoost model for gasoline model classification, and the remaining 122 samples are classified correctly, with an accuracy rate of 96.83%. In Fig. 10(b), 10 samples are misclassified in the SSA-XGBoost model, and its accuracy is 92.06, which is a decrease of 4.77% compared to the IMPA-XGBoost model. In Fig. 10(c), there are 15 samples misclassified in the PSO-XGBoost model, and the CA is only 88.10%. It indicates that the IMPA-XGBoost model has higher gasoline model CA, which further validates the superiority of the IMPA-XGBoost model in gasoline quality detection.

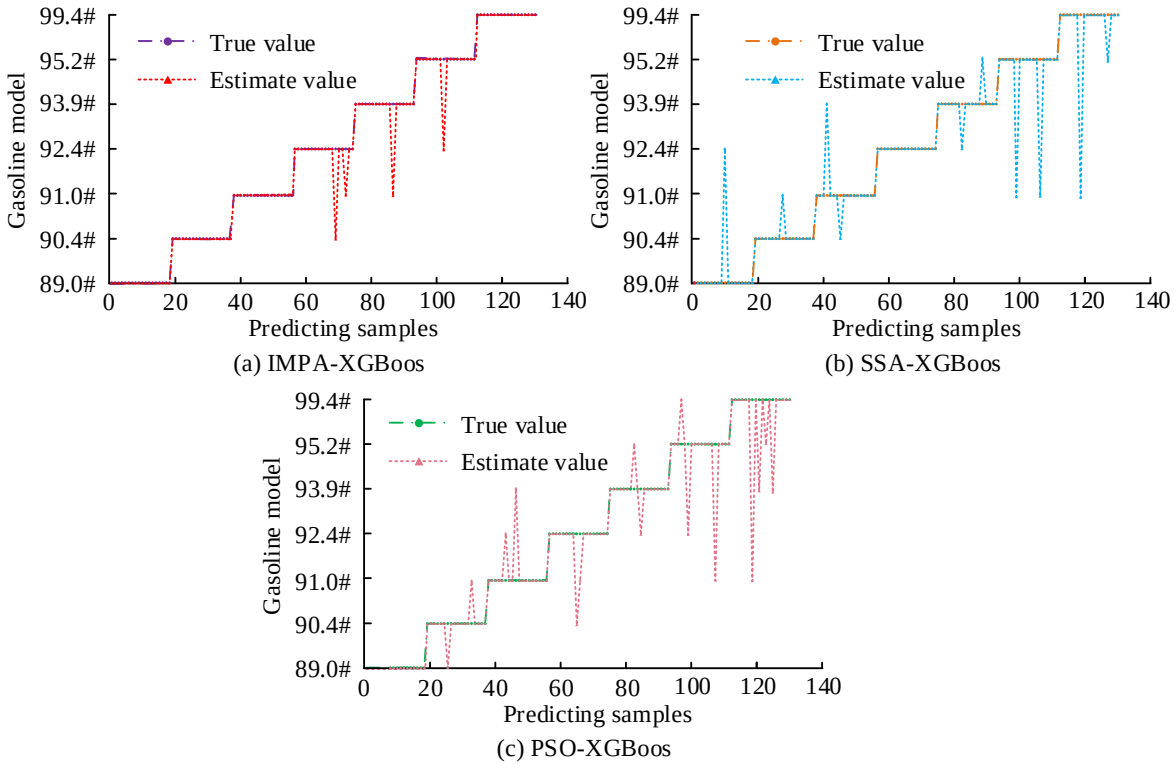

Figure 10: Classification accuracy of gasoline models by various models.

To verify the model's generalization ability, an additional 20 new gasoline samples are introduced for testing. These samples included 92 and 95 aviation gasoline produced by different refineries, as well as experimental samples containing new additives. The experimental results are shown in Table 5. Table 5 shows that the IMPA XGBoost model achieves a CA of 93.5% for newly added samples. This result is significantly better than those of the PSO XGBoost and SSA XGBoost models. This is due to the robust extraction of core quality features by the RAP feature selection algorithm and the optimization of XGBoost parameters by the IMPA. These features enable the algorithm to effectively identify unseen fuel feature variations.

Table 5: Model generalization ability test results.

Model	Number of test samples	Correct classification number	Classification accuracy (%)
IMPA-XGBoost	20	18	93.5%
PSO-XGBoost	20	17	87.2%
SSA-XGBoost	20	18	89.1%

4 Discussion

In order to achieve quality inspection of aviation gasoline, a gasoline quality inspection model based on IMPA-XGBoost algorithm was proposed. Compared with WOA XGBoost, the IMPA XGBoost model in this study improved AUC value by 0.0592 and accuracy by 8.73%. The initialization of the population by the logistic chaotic mapping in the IMPA enabled the algorithm to explore the solution space more widely in the early stages of the search, thus avoiding falling into local optima. The adaptive t-distribution operator enhanced the algorithm's ability to mine the optimal solution in the later stages of the search. The RAP method effectively removed redundant information between features while preserving key features. It accomplished this by combining the Relief-F algorithm with the PCC method. Compared with the Relief-F algorithm alone, it had significantly improved the accuracy and efficiency of feature selection. Deploying an artificial intelligence-based aviation gasoline quality inspection system was highly significant in real-world combat environments. The system did not need expensive and complex testing equipment, and could quickly and accurately complete the gasoline quality testing task. It was conducive to improving the efficiency of aviation gasoline quality testing, reducing testing costs and ensuring flight safety. This system could serve as an important supplement to the existing testing process in places such as airport oil depots and airline maintenance departments. By quickly screening gasoline samples with quality issues, it provided clearer targets for subsequent precise testing.

Integrating the proposed artificial intelligence detection system with existing chemical detection methods improved the efficiency and accuracy of testing the quality of aviation gasoline. Artificial intelligence detection systems, for example, could supplement existing methods by quickly screening gasoline samples for quality issues and providing clearer objectives for subsequent chemical testing. Meanwhile, chemical detection methods could further validate and confirm the results of artificial intelligence testing, ensuring the reliability of the test results. One possible integration solution was to use an artificial intelligence detection system based on IMPA-XGBoost for preliminary screening of a large number of gasoline samples in the aviation gasoline quality inspection process. This system could quickly determine whether the samples meet quality standards. For samples with doubts about the results of artificial intelligence testing, precise analysis could be conducted using existing chemical testing methods to ultimately determine the quality status of gasoline.

5 Conclusion

To realize the quality detection of aviation gasoline, the study introduced an advanced artificial intelligence automated system and proposed a gasoline quality detection model based on IMPA-XGBoost algorithm. The results indicated that the accuracy of the RAP-based feature selection algorithm was as high as 97.26% on average, the average recall was as high as 94.86%, and the average F1 value was as high as 96.23%. The reason for this was that the RAP-based feature selection algorithm was able to reduce the effect of redundant information and noise by optimizing the feature set. This enabled the model to better capture important information related to gasoline quality throughout the testing phase. After feature selection using the RAP algorithm, the average running time of the gasoline detection model was only 386.69ms, which was reduced by 362.81ms compared to the Relief-F algorithm. In contrast, the average running time of the gasoline detection model was as high as 160.38ms in the blank group where no feature selection was performed. This was due to the RAP algorithm's ability to effectively filter out the most discriminative features, reducing the amount of data the model needed to process and thus reducing the computational burden and running time. The results indicated that the gasoline quality detection model based on the IMPA-XGBoost algorithm performed excellently in detecting the quality of aerospace gasoline, demonstrating high efficiency and stability.

However, there are certain limitations to the research. First, optimizing the IMPA parameters requires experience. Additionally, there are computational resource challenges in embedded deployment. Second, the compatibility of the model with other spectral detection techniques has not been validated. Future research will develop an end-to-end model that processes raw spectra and uses lightweight algorithms to enable real-time embedded detection. At the same time, consider

collaborating with the industry to carry out multi-scenario field verification and promote the development of an AI detection standard system.

References

[1] A. Bauen, N. Bitossi, L. German, A. Harris, and K. Leow, "Erratum: Sustainable aviation fuels: status, challenges and prospects of drop-in liquid fuels, hydrogen and electrification in aviation," Johnson Matthey Technology Review, vol. 64, no. 3, pp. 263-278, 2020. https://doi.org/10.1595/205651321X16248677698588

[2] A. Anderson, A. Karthikeyan, C. Ramesh Kumar, S. Ramachandran, and T. R. Praveenkumar, "Lowest emission sustainable aviation biofuels as the potential replacement for the Jet-A fuels," Aircraft Engineering and Aerospace Technology, vol. 93, no. 3, pp. 502-507, 2021. https://doi.org/10.1108/AEAT-07-2020-0135

[3] B. W. Kolosz, Y. Luo, B. Xu, M. M. Maroto-Valer, and J. M. Andresen, "Life cycle environmental analysis of 'drop in'alternative aviation fuels: A review," Sustainable Energy Fuels, vol. 4, no. 7, pp. 3229-3263, 2020. https://doi.org/10.1039/C9SE00788A

[4] Y. Zou, " Prediction of mine gas content using optimized backpropagation neural networks and genetic algorithms for fire prevention," Informatica, vol. 48, no. 16, pp. 113 – 124, 2024. https://doi.org/10.31449/inf.v48i16.6317

[5] D. A. Velandia Cárdenas, E. J. López Pulgarín, and J. Iván Sofrony, "Data-driven fault detection in a thermocouple network using neighboring redundancy, XGBoost classifier, and up-down counter," IEEE Sensors Journal, vol. 24, no. 4, pp. 5215-5223, 2024. https://doi.org/10.1109/JSEN.2023.3342614

[6] J. S. Eom, L. K. Hee, and W. S. Cho, "A classification model for customs clearance inspection results of imported aquatic products using machine learning techniques," The Journal of Bigdata, vol. 8, no. 1, pp. 157-165, 2023. https://doi.org/10.36498/kbigdt.2023.8.1.157

[7] S. Zhang, X. Zhu, B. Anduv, X. Jin, and Z. Du, "Fault detection and diagnosis for the screw chillers using multi-region XGBoost model," Science and Technology for the Built Environment, vol. 27, no. 5, pp. 608-623, 2021. https://doi.org/10.1080/23744731.2021.1877966

[8] X. Chen, D. Yu, X. Fan, L. Wang, and J. Chen, "Multiclass classification for self-admitted technical debt based on XGBoost," IEEE Transactions on Reliability, vol. 71, no. 3, pp. 1309-1324, 2021. https://doi.org/10.1109/TR.2021.3087864

[9] Y. Qiu, J. Zhou, M. Khandelwal, H. Yang, P. Yang, and C. Li, "Performance evaluation of hybrid WOA-XGBoost, GWO-XGBoost and BO-XGBoost models to predict blast-induced ground vibration," Engineering with Computers, vol. 38, no. 5, pp. 4145-4162, 2022. https://doi.org/10.1007/s00366-021-01393-9

[10] A. Asselman, M. Khaldi, and S. Aammou, "Enhancing the prediction of student performance based on the machine learning XGBoost algorithm," Interactive Learning Environments, vol. 31, no. 6, pp. 3360-3379, 2023. https://doi.org/10.1080/10494820.2021.1928235

[11] M. Ramezani, D. Bahmanyar, and N. Razmjooy, "A new improved model of marine predator algorithm for optimization problems," Arabian Journal for Science and Engineering, vol. 46, no. 9, pp. 8803-8826, 2021. https://doi.org/10.1007/s13369-021-05688-3

[12] M. Abd Elaziz, A. A. Ewees, D. Yousri, L. Abualigah, and M. A. Al-Qaness, "Modified marine predators' algorithm for feature selection: Case study metabolomics," Knowledge and Information Systems, vol. 64, no. 1, pp. 261-287, 2022. https://doi.org/10.1007/s10115-021-01641-w

[13] Q. He, Z. Lan, D. Zhang, L. Yang, and S. Luo, "Improved marine predator algorithm for wireless sensor network coverage optimization problem," Sustainability, vol. 14, no. 16, pp. 9944, 2022. https://doi.org/10.3390/su14169944

[14] H. Jia, K. Sun, Y. Li, and N. Cao, "Improved marine predators' algorithm for feature selection and SVM optimization," KSII Transactions on Internet and Information Systems (TIIS), vol. 16, no. 4, pp. 1128-1145, 2022. https://doi.org/10.3837/tiis.2022.04.003

[15] T. C. Uyan, K. Otto, M. S. Silva, P. Vilaça, and E. Armakan, "Industry 4.0 foundry data management and supervised machine learning in low-pressure die casting quality improvement," International Journal of Metalcasting, vol. 17, no. 1, pp. 414–429, 2023. https://doi.org/10.1007/s40962-022-00783-z

[16] Z. Chen, "Tax risk early warning system for SMEs using auto encoder-backpropagation neural network with genetic algorithm optimization," Informatica, vol. 49, no. 6, 2025. https://doi.org/10.31449/inf.v49i6.6830

[17] J. Joseph and K. Kartheeban, "Visualizing the full spectrum optimization of K-nearest neighbors from data preprocessing to hyperparameter tuning and K-fold validation for cardiovascular disease prediction," Informatica, vol. 49, no. 2, 2025. https://doi.org/10.31449/inf.v49i2.7774

[18] H. W. Xu, W. Qin, and Y. N. Sun, "An improved XGBoost prediction model for multi-batch wafer yield in semiconductor manufacturing," IFAC-PapersOnLine, vol. 55, no. 10, pp. 2162-2166, 2022. https://doi.org/10.1016/j.ifacol.2022.10.028

[19] H. Mokayed, T. Z. Quan, L. Alkhaled, and V. Sivakumar, "Real-time human detection and counting system using deep learning computer vision techniques," Artificial Intelligence and Applications, vol. 1, no. 4, pp. 221-229, 2023. https://doi.org/10.47852/bonviewAIA2202391

[20] C. Xu, X. Liu, H. Wang, Y. Li, W. Jia, W. Qian, and F. Xue, “A study of predicting irradiation-induced transition temperature shift for RPV steels with XGBoost modeling,” Nuclear Engineering and Technology, vol. 53, no. 8, pp. 2610-2615, 2021. https://doi.org/10.1016/j.net.2021.02.015

[21] M. Wang, X. Song, S. Liu, X. Q. Zhao, and N. R. Zhou, “A novel 2D log-logistic–sine chaotic map for image encryption,” Nonlinear Dynamics, vol. 113, no. 3, pp. 2867 – 2896, 2025, https://doi.org/10.1007/s11071-024-10331-5.